# High-Energy Ion Generation During Difference-Frequency ICRF Wave Heating in GAMMA 10/PDX*)

Yudai SUGIMOTO, Mafumi HIRATA, Yousuke NAKASHIMA, Makoto ICHIMURA, Doyeon KIM, Takaaki KOZAWA, Shunya ENDO, Ryo KOBAYASHI, Ryuya IKEZOE[1)], Naomichi EZUMI, Satoshi TOGO, Masayuki YOSHIKAWA, Junko KOHAGURA and Mizuki SAKAMOTO

*Plasma Research Center, University of Tsukuba, Tsukuba 305-8577, Japan*
[1)]*Research Institute for Applied Mechanics, Kyushu University, Kasuga 816-8580, Japan*

(Received 29 December 2022 / Accepted 28 August 2023)

One of the greatest challenges of simulating the high heat flux on the divertor in linear plasma devices is the achievement of ion temperatures of > 100 eV under high densities ($\geq 10^{19}\,\mathrm{m}^{-3}$). The slow wave in the ion cyclotron range of frequency has been employed for ion heating in GAMMA 10/PDX and demonstrated its high efficiency at middle densities of $10^{18}\,\mathrm{m}^{-3}$. However, at high densities ($\geq 10^{19}\,\mathrm{m}^{-3}$), exciting the slow wave in the center of the plasma by external antennas becomes challenging. Alternatively, we have demonstrated the excitation of the difference-frequency (DF) slow wave using two high-density-applicable fast waves. In this study, we first applied the charge-exchange neutral particle analyzer (CX-NPA) to a DF wave heating experiment. Even when the bulk temperature did not increase significantly, the high-energy ions in the > 0.5 keV range were measured during the experiment. Such high-energy ions were only measured in the central line of sight of CX-NPA, indicating that the power deposition from the DF wave was largely centered and differed greatly from the normal heating scheme using external antennas. This result will motivate further pursue of exploiting nonlinearity of plasma media to produce different heating accessibilities.



Keywords: ICRF, ion heating, slow wave, fast wave, difference-frequency wave, high density, charge-exchange neutral particle analyzer, mirror plasma, GAMMA 10/PDX, divertor simulation

DOI: 10.1585/pfr.18.2402084

## 1. Introduction

To ensure the availability of a fusion reactor, the expected long-term plasma-wall interaction (PWI) in the divertor of a DEMO reactor under high-temperature and high-particle-flux conditions must be investigated. During such investigations, linear plasma devices have been utilized owing to their good operability and accessibility for plasma measurements. However, no known linear plasma device can simultaneously satisfy the aforementioned features [1]. Although considerably high ion temperatures (100 eV) are required to completely simulate a DEMO reactor, most existing steady-state, high-density linear plasma devices exhibit low ion temperatures. Therefore, an efficient method for increasing the ion temperatures of such divertor simulation devices is desirable.

Ion cyclotron range of frequency (ICRF) waves are widely employed for the production and heating of plasma on fusion experiment devices. They are particularly effective in mirror-configuration ion heating at middle densities. The Alfvén slow waves in ICRF excited by the magnetic high-field side are propagated toward the low-field side and are absorbed by ions via cyclotron resonance. High ion heating efficiency can be achieved by the Doppler-broadened wide resonance region and low gradient with the magnetic-field-strength resonances; this is called beach heating. In the GAMMA 10/PDX tandem mirror, hydrogen plasma is solely produced and heated by ICRF waves [2, 3]. Therein, ion temperatures of several keV perpendicular to the magnetic field line, as well as the strong anisotropy in the pitch-angle distribution of the ions, have been routinely observed in the mirror-confinement region, with an electron density of $2 \times 10^{18}\,\mathrm{m}^{-3}$ [4, 5]. PWI and plasma-gas interactions have been studied in divertor-simulation modules using the end-loss plasmas exhibiting high ion temperatures [6–8]. Thus, ICRF slow wave heating might represent the first candidate heating method in linear plasma devices. However, the excitation of slow waves to the central region of a plasma using external antennas in the cold-plasma-approximation limit could be challenging at high densities ($> 10^{19}\,\mathrm{m}^{-3}$) [9]. Conversely, kinetic Alfvén waves are excited at finite temperatures, even in high-density plasmas; the heating effect was recently reported in Proto-MPEX [10].

As has been experimentally demonstrated in GAMMA 10/PDX, the excitation of two fast Alfvén

*author's e-mail: sugimoto_yudai@prc.tsukuba.ac.jp*
*) This article is based on the presentation at the 31st International Toki Conference on Plasma and Fusion Research (ITC31).

waves with frequencies, $f_1$ and $f_2$, induces the nonlinear excitation of a slow Alfvén wave with the difference frequency ($|f_1 - f_2|$) in the center of a plasma [11, 12]; the process is called difference-frequency (DF) wave heating. Although exhibiting low efficiency, DF wave heating can be a candidate for future heating methods when other methods become challenging. As the DF heating experiment involves significant changes in the heating system, it is accompanied by numerous restrictions that would prevent the execution of many experiments; moreover, the excitation conditions have not yet been clarified. However, we have markedly increased diamagnetism, and this corresponds to increased ion temperatures [13].

In this paper, we report the first experimental observation of the generation of high-energy ions in the > 0.5 keV range during DF wave heating in the GAMMA 10/PDX central cell, as well as the neutral particle measurement. Section 2 presents the experimental settings for the DF wave heating experiment, as well as the specifications of the charge-exchange neutral particle analyzer (CX-NPA) in GAMMA 10/PDX. Section 3 presents the data of the generated high-energy ions. Sections 4 and 5 present the discussion and summary of the study, respectively.

## 2. Experimental Device

### 2.1 GAMMA 10/PDX and the ICRF system

GAMMA 10/PDX comprises an axisymmetric central mirror cell, anchor cells with minimum-B coils, and plug/barrier cells with axisymmetric mirrors. Its axial length is 27.1 m, lying along the east, and west directions. Hereafter, the prefixes, E-, and W-, will be used to denote the east and west sides, respectively. The central cell confining the main plasma exhibits an axial length of 5.6 m. The magnetic flux density in the midplane of the central cell was 0.41 T, and the mirror ratio was 4.9. The magnetic field was almost uniform in the radial direction. Further, the diameter of the plasma in the central cell was ~ 0.36 m. Pure hydrogen plasma was initiated by a plasma gun and built up using the ICRF waves together with gas puffing. Figure 1 shows the $z$-axis profiles of the magnetic field strength and ion cyclotron frequency ($\omega_{ci}$), as well as the location of the ICRF antennas and diagnostics in the central cell. Here, the $z$-axis is set at the center of the magnetic field line, and the origin ($z = 0$) is set at the midplane of the central cell.

Three types of ICRF antennas were used for the DF wave heating experiments: the Nagoya Type-III (Type-III), double-half-turn (DHT), and double-arc-type (DAT) antennas. The Type-III antennas were installed near both throats of the central cell (at $z = \pm 2.2$ m) [3] and comprised two electrodes, which were 0.25 m in the magnetic field direction and 0.18 m across the magnetic field. The radiofrequency (RF) current flows parallel to the magnetic field lines. In GAMMA 10/PDX, they are used to excite fast waves with azimuthal mode number, $m = +1$. The frequencies of the E- and W-Type-III antennas were set to 9.9 and 10.3 MHz, respectively, facilitating the production of plasma in the central cell and magnetohydrodynamic stabilization in the anchor cells [14]. The DHT antennas were installed at $z = \pm 1.7$ m. They comprise two electrodes that loop around the plasma, and the RF current flows perpendicular to the magnetic-field lines. As shown in Fig. 1, $\omega_{ci}$ is ~ 6.36 MHz near the midplane of the central cell. In normal discharges, the frequency of DHT antennas is set to 6.36 MHz ($m = -1$) to facilitate effective beach heating using the slow wave. The DAT antennas, which are similar to the DHT ones and shaped to fit the plasma cross-section at the antenna location, were installed in the anchor cells. E- and W-DAT were also set to the same frequencies (9.9 and 10.3 MHz) as those of the E- and W-Type-III antennas, respectively. A higher-than-usual-density plasma could be generated by controlling the phase difference between the Type-III and DAT antennas [15, 16].

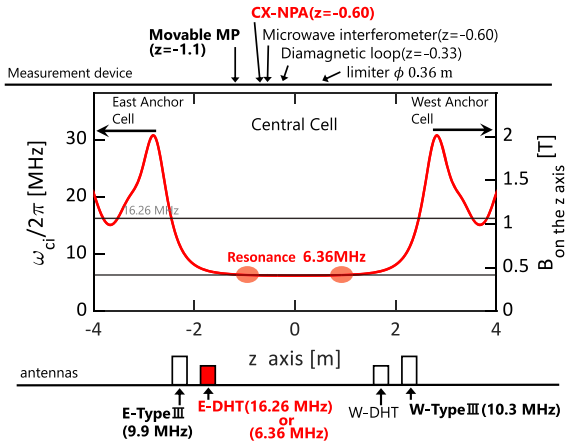


Fig. 1 Z-axis profiles of the magnetic field strength and ion cyclotron frequency in the central cell, as well as the locations of the ICRF antennas and diagnostics. The 6.36 and 16.26 MHz frequencies are indicated.

The DF wave heating experiments did not use 6.36 MHz for DHTs. Rather, the E-DHT frequency was set to 16.26 MHz. The wave with a 6.36 MHz frequency was excited as the DF wave between the waves with 16.26 and 9.9 MHz in the central cell. At the E-DHT location, the 16.26 MHz frequency satisfied $\omega/\omega_{ci} > 1$, where $\omega$ is the wave frequency. Thus, the wave with 16.26 MHz was excited as a fast wave exerting a negligible ion-heating effect. Only the DF wave with 6.36 MHz was expected to cause ion heating. To excite the DF wave as a slow wave with $m = -1$, the fast wave with 16.26 MHz was excited with $m = 0$ by changing the phasing of the two electrodes, as well as adjusting the matching circuit. It is known that the fast wave with $m = 0$ cannot propagate in an ideal cylindrical plasma below a cutoff frequency, which is higher than $\omega_{ci}$ [17]. Thus, higher densities could favor this experiment.

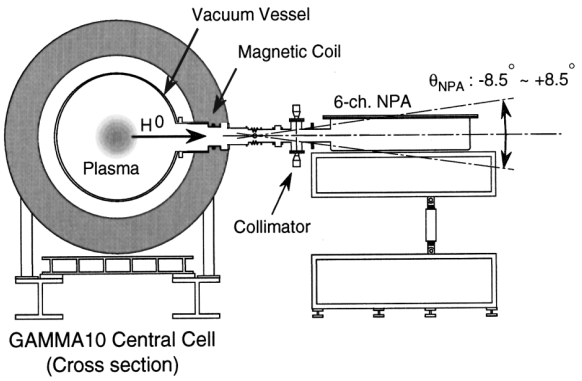


Fig. 2 Schematic of CX-NPA that was installed perpendicular to the magnetic axis in GAMMA 10/PDX [20].

### 2.2 Charge-exchange neutral particle analyzer

CX-NPA is a valuable diagnostic for measuring ion temperatures in tandem mirror devices. It has been used to study the ion energy balance and heating mechanisms in GAMMA 10/PDX [18, 19]. Figure 2 shows the schematic of CX-NPA, which was installed near the midplane of the central cell ($z = -0.6$ m) in GAMMA 10/PDX. The fast neutral particles with a pitch angle ($\sim 90°$) were detected. The viewing angle of CX-NPA can be scanned to radially change the measurement position. Here, we set the viewing angle to allow us to measure at $r_{cc} = 2.5$ and 5.0 cm ($r_{cc}$ denotes the radius of the central cell). In GAMMA 10/PDX, neutral hydrogen atoms, and molecules can readily penetrate the plasma, as the averaged plasma density is only a few $10^{18}$ m$^{-3}$. The ion temperature is calculated by considering the effect of the finite Larmor radius of the ions [21]. Multiple plasma discharges were employed to reduce the statistical errors of the detected high-energy neutral-particle counts in the measurement.

## 3. Difference-Frequency Wave Heating Experiment

Figure 3 shows the typical time evolution of the plasma parameters during the DF wave heating discharge. For comparison, the waveforms of the discharge without the 16.26 MHz wave are shown together. The plasma was produced from 50 to 250 ms. The E- and W-DAT antennas were powered at 100 ms, and additional gas was injected from 180 ms to increase the density, thus impacting the 16.26 MHz excitation and DF waves. Accordingly, the base plasma exhibiting three stages of density changes was produced (Fig. 3 (c)). The radial profiles of the electron density during the DF wave experiments were obtained by the Abel transform of the line-integrated densities measured with the movable microwave interferometer. The profiles at two-time slices exhibited a rounded peak in the center (Fig. 4). The 16.26 MHz excitation did not significantly affect the visible parameters. Unfortunately, the electron-density profile of the injected without-16.26 MHz wave was not measured. Both line-integrated densities were almost same (Fig. 3 (c)). The electron temperatures at $t = 130$ and 230 ms, measured by the Thomson scattering system at $z = 0.6$ m and $r_{cc} = 0$ cm, were approximately 50, and 30 eV, respectively, for both cases, and the energy distributions of the end-loss ions did not exhibit any change when the additional RF of 16.26 MHz was applied. Although the difference between the diamagnetism of the with- and without-16.26 MHz waves in this experiment was unfortunately not significant, the 6.36 MHz DF wave was surely excited, as confirmed by the insertable magnetic probe.

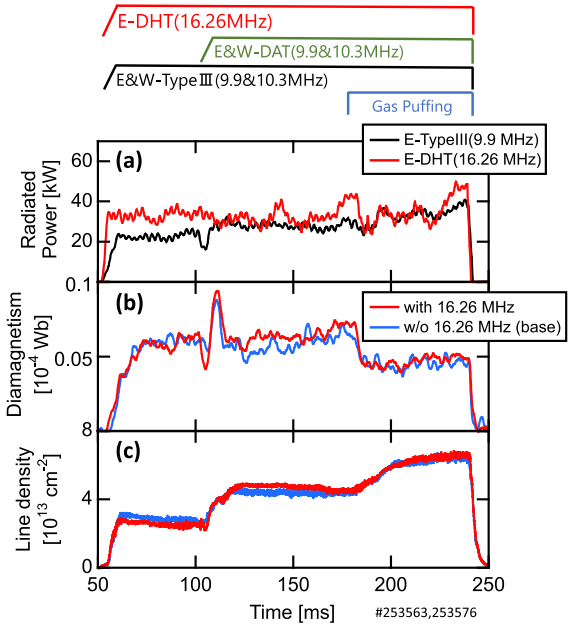


Fig. 3 Typical time evolution of the RF pulses and gas injection (top): (a) radiated power of 9.9 and 16.26 MHz RF from the antennas, (b) diamagnetism, and (c) line density in the central cell. In (b) and (c), the red and blue lines denote the discharge with and without the applied 16.26 MHz wave, respectively.

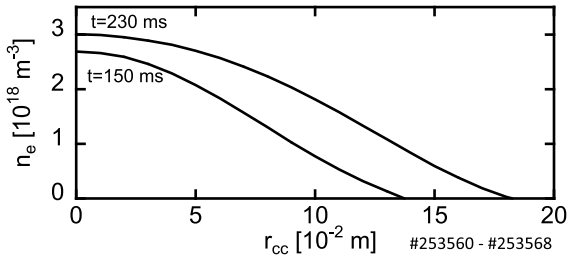


Fig. 4 Reconstructed radial profiles of the electron density at t = 150 and 230 ms for the DF wave-heating discharge shown in Fig. 3.

Figure 5 shows the time evolutions of the magnetic fluctuations at 9.9, 16.26 and 6.36 MHz, which were measured by the insertable magnetic probe installed at $z =$

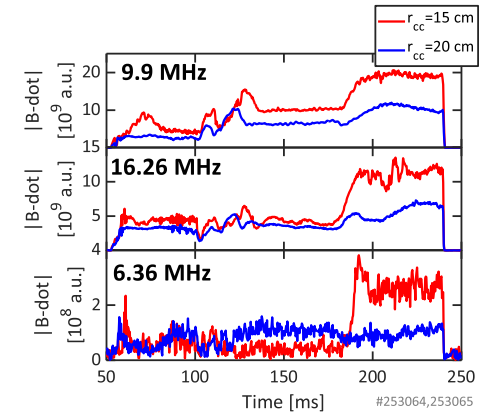


Fig. 5 Time evolution of the magnetic fluctuations measured by the movable magnetic probe that was inserted into the plasma. The red and blue lines indicate the measurement results at $r_{cc}$ = 15 and 20 cm, respectively.

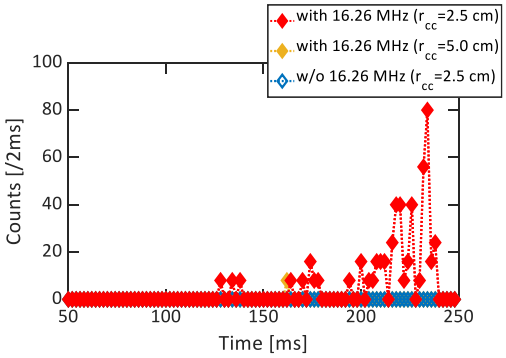


Fig. 6 Time evolution of the sum of the counts of charge-exchange neutral particles at 0.5 - 4.0 keV.

−1.1 m. Figure 5 shows that the 9.9 MHz waves were excited more strongly as the density increased; they were more strongly excited at $r_{cc}$ = 15 cm than at the edge. Conversely, the 16.26 MHz wave remained at the same level until 180 ms, after which it drastically increased by approximately 2.5 times at $r_{cc}$ = 15 cm. This is partly because the $m$ = 0 fast wave was less likely excited at low densities. The DF wave at 6.36 MHz exhibited a further drastic intensity change, jumping up from 180 ms, when the density was further increased by gas puffing. Notably, the 6.36 MHz intensity at the edge maintained its level despite the noticeable increase observed on the inside. Therefore, the behavior of the DF wave was dominated by nonlinearity and was complicated.

Figure 6 shows the time evolution of the sum of the counts of the charge-exchange neutral particles in the energy range from 0.5 to 4.0 keV, as measured with CX-NPA. Although the charge-exchange neutral particles were not detected at all at any period in the without-16.26 MHz-wave case, significant counts were detected when applying the 16.26 MHz wave, particularly after 200 ms, when the density was relatively high; the DF wave exhibited remarkable excitation. The charge-exchange neutral particle flux, $\Gamma_{CX}$, was proportional to $N_i f(E) N_0 \langle \sigma_{CX} v_i \rangle$, where $N_i$ is the ion density, $f(E)$ is the ion-energy distribution function, $N_0$ is the neutral-particle density, $\sigma_{CX}$ is the charge-exchange reaction cross-section, and $v_i$ is the ion velocity [21]. As the differences among the densities and other measured plasma parameters (diamagnetism, $T_e$, end-flux, etc.) were not very significant under both conditions, it would be reasonable to attribute the remarkable difference between the numbers of counts of the with- and without-16.26 MHz waves to the difference in $f(E)$. No counts were measured in the absence of 16.26 MHz even after 200 ms, where the density was as high as that in the presence of counts for the 16.26-MHz-wave discharges; moreover, as much gas puffs were applied as in the presence of counts for the 16.26-MHz-wave discharges (Fig. 6). Therefore, this observation indicates that $f(E)$ in the measured energies was significantly increased by the application of the 16.26 MHz wave. These results, as well as that of the wave measurements, revealed that the DF wave could generate high-energy ions in the > 0.5 keV range.

Additionally, Fig. 6 shows that the number of counts was significant and insignificant at $r_{cc}$ = 2.5 and 5.0 cm, respectively, in the DF wave heating. Although the wave measurements using a reflectometer and magnetic probe in the central region could not be conducted during the DF wave heating experiment, this result strongly indicates the difference between the radial profiles of the DF and external-antennas-excited waves. The extant microwave reflectometry measurements indicated that the normal slow wave excited by the external DHT antenna exhibited significant amplitude in the peripheral region rather than in the central region [22, 23].

## 4. Discussion

We conducted a normal heating experiment using the 6.36 MHz slow wave that was excited by an E-DHT antenna with reduced powers, i.e., the frequency of E-DHT was changed from 16.26 to 6.36 MHz. Figure 7 shows the time evolution of the plasma parameters. Employing the CX-NPA counts (Fig. 7 (d)), the data of the DF wave heating were plotted for comparison. Radiated powers of only ∼ 15 kW, the diamagnetism was higher than in the case of the DF wave heating. The plasma densities were in a similar range. Although the number of counts for the high-energy ions was significant in the normal heating discharge, it suddenly decreased when the density was increased by additional gas puffs (Fig. 7 (d)). The ion temperature decreased with the decreasing diamagnetism. This is caused by the combination of the enhanced charge-exchange loss of ion energies and reduced wave power in the center. However, as already described (Fig. 6), the number of counts for DF wave heating tended to increase under such conditions, with increased electron, and neutral particle densities.

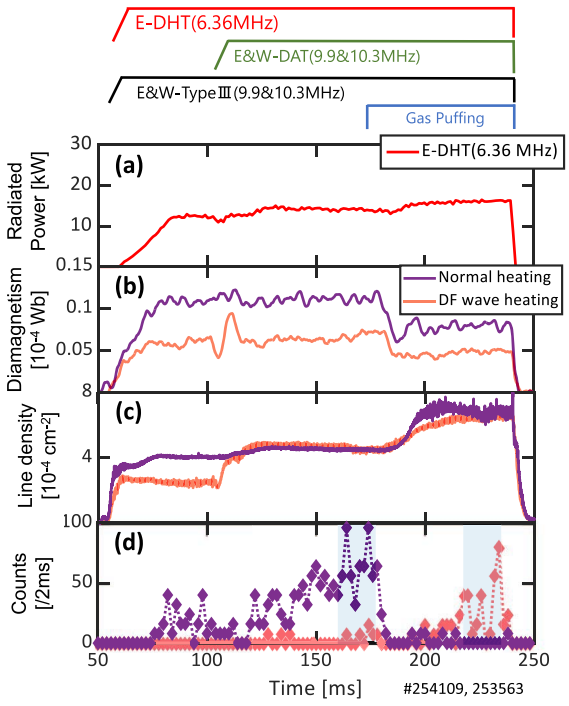


Fig. 7 Waveforms of the RF pulses and gas injection: (a) radiated power of 6.36 MHz RF from the antenna, (b) diamagnetism, (c) line density, and (d) the sum of the CX-NPA counts in the energy range of 0.5 - 4.0 keV at $r_{cc}$ = 2.5 cm in the central cell. In panel (d), the purple and light-red lines denote the normal and DF wave heating, respectively. The light-blue region denotes the periods for analyzing the energy spectra shown in Fig. 8.

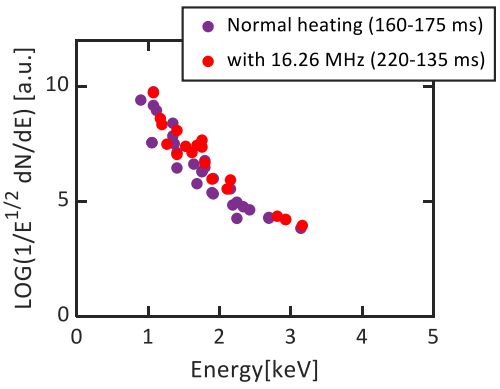


Fig. 8 Energy spectra obtained by the with-CX-NPA set at $r_{cc}$ = 2.5 cm. Data are recorded from 220 - 235 ms for the DF wave heating (red) and 160 - 175 ms for the normal heating experiment (purple).

Figure 8 shows the obtained energy spectra at $r_{cc}$ = 2.5 cm for both experiments. The ion-energy spectra were very close in the measured energy range even though the diamagnetism in the DF wave heating discharge was clearly lower than that in the normal heating discharge. Therefore, together with the experimental result that did not exhibit CX-NPA counts at $r_{cc}$ = 5.0 cm during the DF wave heating, this comparison indicates the difference in the radial profiles of the ion temperature; the typical round-top profile for the normal wave and sharply peaked profile for the DF wave heating were inferred.

The difference between our DF wave heating experiment and previous related experiments, which indicated increased diamagnetism [13], remains unclear. As previously explained via magnetic measurements, the excitation of the DF wave suffered from nonlinear features; thus, a slight difference in the impedance matching of the 16.26 MHz system and coupling with plasma may have produced a large difference in the DF wave intensity, as well as the bulk-heating effect. The excitation of the $m = 0$ fast wave represents a new attempt for these DF wave heating experiments, and further adjustments can facilitate ion-energy distributions for a DF wave heating discharge with significant bulk ion heating.

## 5. Summary

As a new ion heating method that applies to high-density linear plasmas, DF ICRF wave heating was proposed and experimentally tested in GAMMA 10/PDX. The magnetic measurements exhibited the strong nonlinearity of the excitation of the DF wave. By applying CX-NPA, we observed that high-energy ions were generated when the DF wave was strongly excited. Such noticeable generation of the high-energy ions was observed only near the center, and it differed greatly from the normal heating scheme where the slow wave with the same frequency as the DF wave was directly excited by the external antenna. Thus, the different heating characteristics, which were attributed to the differences in the excitation methods, were demonstrated. This result will serve as a basis for further exploration of the nonlinearity of plasma media to produce different heating accessibilities. The quantitative clarification of the excitation conditions of the DF wave, as well as the heating efficiency, require further elaborate experiments, together with detailed measurements suited to this experiment, and this is the scope of a future study.

## Acknowledgment

The authors acknowledge the members of the Plasma Research Center at the University of Tsukuba for their collaboration. This work was partly supported by the bidirectional collaborative research program of the National Institute for Fusion Science, Japan (NIFS21KUGM166, NIFS22KUGM173).

[1] N. Ohno, Plasma Phys. Control. Fusion **59**, 034007 (2017).
[2] M. Ichimura *et al.*, Nucl. Fusion **28**, 799 (1988).
[3] M. Ichimura *et al.*, Plasma Phys. Reports **28**, 727 (2002).
[4] R. Katsumata *et al.*, Jpn. J. Appl. Phys. **30**, 854 (1991).
[5] M. Ichimura *et al.*, Jpn. J. Appl. Phys. **31**, 2249 (1992).
[6] Y. Nakashima *et al.*, Nucl. Fusion **57**, 116033 (2017).
[7] M. Sakamoto *et al.*, Nucl. Mater. Energy **12**, 1004 (2017).
[8] H. Gamo *et al.*, Plasma Fusion Res. **16**, 2402041 (2021).

[9] R. Ikezoe *et al.*, Plasma Fusion Res. **14**, 2402003 (2019).
[10] R.H. Goulding *et al.*, Phys. Plasmas **30**, 013505 (2023).
[11] M. Ichimura *et al.*, J. Plasma Fusion Res. SERIES **8**, 893 (2009).
[12] R. Sekine *et al.*, Plasma Fusion Res. **14**, 2402011 (2019).
[13] H. Kayano *et al.*, Plasma Fusion Res. **16**, 2402045 (2021).
[14] M. Inutake *et al.*, Phys. Rev. Lett. **65**, 27 (1990).
[15] S. Sumida *et al.*, Fusion Sci. Technol. **68**, 136 (2017).
[16] R. Ikezoe *et al.*, Fusion Sci. Technol. **68**, 63 (2017).
[17] F.J. Paoloni, Phys. Fluids **18**, 640 (1975).
[18] Y. Nakashima *et al.*, Fusion Eng. Des. **34-35**, 555 (1997).
[19] M. Shoji *et al.*, Plasma Phys. Control. Fusion **43**, 761 (2001).
[20] Y. Nakashima *et al.*, Rev. Sci. Instrum. **70**, 849 (1999).
[21] M. Shoji *et al.*, J. Phys. Soc. Jpn. **65**, 2846 (1996).
[22] R. Ikezoe *et al.*, AIP Conference Proceedings **1771**, 050002 (2016).
[23] R. Ikezoe *et al.*, JINST **12**, C12017 (2017).